2025 IEEE/SICE International Symposium on System Integration (SII)
January 21-24, 2025, Munich, Germany

Pre-touch Deformation Estimation of Soft Robotic Gripper based on Camera Image

Ryogo Kai[1], Yuzuka Isobe[1], Sarthak Pathak[2], and Kazunori Umeda[2]

***Abstract*— Soft robotic grippers are highly adaptable to various objects because they can deform and fit object shapes. However, grasping stability may change owing to the posture of the gripper while grasping an object. For a stable grasp, it is necessary to estimate the grasping posture before the grasp, namely pre-touch estimation. In particular, for soft robotic grippers, an important factor in the grasping posture is gripper deformation. In previous studies, pre-touch estimation was researched only for rigid grippers without considering deformation, and the stability of grasping an object using soft grippers was evaluated after grasping. The deformation of the gripper depends on the intrinsic characteristics of the gripper deformation (e.g., stiffness) and the contact positions between the gripper and object, that is, how the gripper can deform and where on the gripper is in contact with the object. Deformation characteristics vary from one gripper to another, and the contact positions change according to the characteristics, gripper location, and object shape. Thus, an estimation method that considers these conditions is required to achieve a pre-touch estimation of the deformation of soft robotic grippers.**

This study presents a vision-based method for estimating the deformation of a soft robotic gripper prior to grasping an object. The entire method is performed before the gripper grasps an object. In the first process, the deformation model that shows the manner in which the gripper can deform is defined using three approaches: discretization of the gripper based on *a model of a serial chain of rigid bodies connected with a spring joint*, the bending angle of the entire gripper, and *piecewise constant curvature*. Next, using an image, the bending angle of the entire gripper is acquired to calibrate the deformation model. Subsequently, the contact points between the gripper and object are predicted by obtaining their contours from an image. Finally, the deformation of the entire gripper is estimated based on the deformation model and predicted contact points. Three experiments were conducted to evaluate the accuracy and versatility of the proposed method with respect to gripper location and object shape.

I. INTRODUCTION

Automation through the introduction of robotic arms and hands is advancing to address labor shortages in factories. Humans are able to grasp various type of objects and easily handle them using their "hand," which is an excellent end-effector. Therefore, a robotic hand that can grasp various objects is required when automating with robots.

To satisfy this requirement, soft robotic grippers have been attracting attention [1], [2]. Unlike conventional robotic grippers, which comprise rigid materials, a soft robotic gripper is composed of soft materials and mechanisms. Because of its softness, a soft robotic gripper can adapt to and fit the shape of objects when grasping, enabling it to grasp various objects. Owing to its high adaptability to the shape of an object, the contact area between the gripper and object is increased. This helps with grasping objects without damaging them, enabling the gripper to grasp soft objects such as food items.

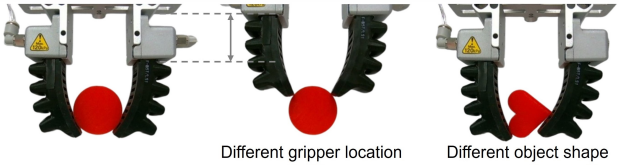

Fig. 1. The differences in the deformation of a soft robotic gripper and that in the contact position due to the gripper location and the object shape.

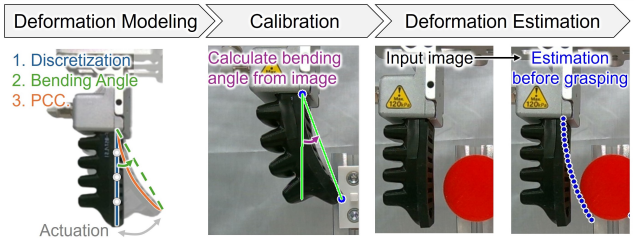

Fig. 2. Overview of the proposed method

However, in practice, the gripper may not grasp an object stably depending on the grasping posture of the soft gripper and may drop or slip the object [3]–[5]. In such a situation, increasing the grasping force and/or re-grasping the object can achieve a stable grasp [6], [7]. Although an object is less likely to be dropped by these post-grasp operations, it may be damaged, particularly in the case of soft objects. To prevent damage, both pre-touch estimation and motion are necessary. The former estimates the grasping posture, and the latter adjusts the gripper location based on the estimation to stably grasp the object, both prior to grasping. To implement this in soft grippers, it is important that the deformation of the gripper is estimated, and the grasping stability in the estimated grasping posture is evaluated. Particularly in the estimation, it should be considered that the deformation depends on not only the deformation characteristics (e.g. stiffness) of the gripper, but also on the contact positions between the gripper and object. The differences in deformation owing to that in the contact position, when changing the gripper location and object shape, are shown in Fig. 1.

Several studies have been conducted on pre-touch estima-

[1]The Precision Engineering Course, Graduate School of Science and Engineering, Chuo University, 1-13-27 Kasuga, Bunkyo-ku, Tokyo, Japan. {kai, isobe}@sensor.mech.chuo-u.ac.jp
[2]The Department of Precision Mechanics, Faculty of Science and Engineering, Chuo University, 1-13-27 Kasuga, Bunkyo-ku, Tokyo, Japan. {pathak, umeda}@mech.chuo-u.ac.jp

tion [8]–[10]. The grasping position was estimated based on the relative position between the rigid robotic gripper and an object before the grasp. However, this approach is limited to rigid grippers because the deformation of the gripper is not considered.

To detect the deformation of a soft gripper, vision-based methods were studied [11], [12]. Meanwhile, methods were proposed to evaluate the grasping stability [3]–[5]. However, these methods are only applicable during grasping. Alternatively, learning-based methods were also developed [13]–[15]; however, their performances may not be guaranteed for untrained objects. Thus, to leverage the adaptability of soft robotic grippers, there is a challenge to estimate the deformation of the grippers before the grasp.

In this study, we propose a method based on camera images for estimating the deformation of a soft robotic gripper before object grasping. Fig. 2 shows the overview of the proposed method. First, a model of the gripper deformation is defined. Three approaches are combined for the modeling: discretization of the gripper by the *model of a serial chain of rigid bodies connected with spring joints* [16], the bending angle of a soft gripper [17], and *piecewise constant curvature* (PCC) [18]. Second, before the estimation, the entire bending angle of the model is calculated only once for calibration. Finally, the gripper deformation was estimated using the deformation model. For the estimation, the contact points between the gripper and object is predicted by considering the model, gripper location, and object shape. Subsequently, the posture of each discretized link of the gripper is calculated. Combining all the postures indicates the deformation of the entire gripper. The effectiveness of the proposed method is verified through experiments at various contact positions by varying the gripper location and object. The novelty and contributions of the proposed method are as follows:

- Providing the grasping posture of a soft robotic gripper before the actual object grasping based on the deformation estimation using a camera image.
- Accurate and versatile estimation under various contact positions by combining a deformation model describing the characterises of the gripper and the prediction of the contact positions.
- No prior learning or knowledge of gripper location and object shape by predicting the contact points between the gripper and the object based on obtaining both contours from an image.

II. RELATED WORKS

Several studies have investigated pre-touch estimation and motion using rigid grippers [8]–[10]. In these studies, the relative position between the gripper and object was measured before the grasp, and the grasping position was estimated. For measurement, proximity sensors [8], [9] or tactile sensors [10] are attached to the surface of the gripper. However, for soft gripper, the grasping position also changed because of the deformation of the gripper, in addition to the relative position before the grasp.

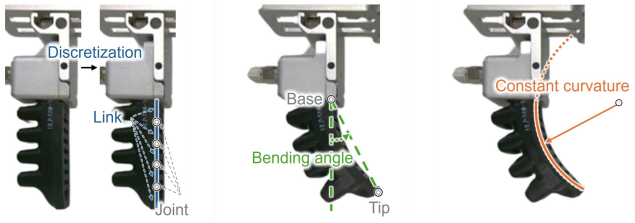

(a) Discretization (b) Bending angle (c) Constant Curvature

Fig. 3. Approaches for deformation estimation

Vision-based methods have been used to determine the deformation of soft grippers. While grasping an object, the markers on the gripper [11] or bending angle [12] were detected using cameras. Methods evaluating the grasp stability based on the grasping force were also proposed [3]–[5]. However, these detections and evaluations can only be performed after the gripper is in contact with an object. Learning-based approaches have been proposed as end-to-end methods [13], [14]. The optimal pose prior to grasping was determined by learning the poses of the gripper and object before grasping and grasping from the pose. Agabiti *et al.* developed a grasping strategy for soft arms with reinforcement learning [15]. The bending of the arm with multiple cabling parts and contact points with objects of specific shapes was learned, and the strategy developed based on them was simulated. Although no model-based estimation or evaluation is required for these approaches, their performance may not be guaranteed for objects with untrained shapes. Therefore, there is a need for an estimation method that can be used without learning or information about the gripper location and the object shape.

III. DEFORMATION MODELS

A. Approaches for modeling

A deformation model is obtained to estimate the deformation of the gripper and show its deformation characteristics. Three approaches are utilized for the modeling. The first is the discretization of the gripper shape using the *model of a serial chain of rigid bodies connected with spring joints* [16]. This approximates the entire gripper with a finite number of rigid links of the same length, as indicated by the blue lines in Fig. 3 (a). The links themselves are not deformed, but are rotated at the joints, as shown by the gray circles in Fig. 3 (a). The second approach introduces the bending angle of a soft gripper [17]. The bending angle is defined as the difference in the angles of the finger before and after deformation. This is calculated as the angle between the vertical axis and the line connecting the base and fingertip, as indicated by the green line in Fig. 3 (b). This angle expresses the extent to which the gripper can deform (i.e., the deformation characteristics), and varies from gripper to gripper. The third is the modeling of the gripper deformation according to *Piecewise Constant Curvature* (PCC) [18]. This design method for continuum robots approximates their shapes as circular arcs with a constant curvature. The soft gripper

focused on in this study is assumed to exhibit reproducibility in terms of opening and closing. Therefore, the deformation problem can be simplified by assuming that the entire gripper deforms according to a constant curvature, as indicated by the orange arc in Fig. 3 (c).

B. Definition of the deformation model

By combining the three approaches introduced in Subsection III-A, a deformation model is obtained. For the model, the posture of each discretized link is calculated using the bending angle and PCC. The length and rotation angle of each link are defined to calculate its posture.

First, the gripper is discretized into a finite number N of rigid links, and the length of each link is calculated. The length of the entire gripper is assumed to remain constant during deformation, as in [16], and is denoted as $L_{gripper}$. Under this assumption, the entire gripper is divided into N rigid links, all of which are equal in length and do not deform. The length L_{link} of each link is calculated as follows:

$$L_{link} = \frac{L_{gripper}}{N} \tag{1}$$

The bending angle of the entire gripper is used to calculate the rotation angle of discretized links. The entire bending angle of the gripper during grasping is assumed to be constant at Θ_{entire}, as indicated by the green arrow in Fig. 4 (a). Subsequently, a constraint is applied such that the gripper deforms according to the PCC model [17]. Under this constraint, the deformation of the gripper can be regarded as an arc with a central angle of $2\Theta_{entire}$ passing through both endpoints P_{base} and P_{tip} of the gripper, as shown by the orange curve in Fig. 4 (a). Next, as shown in Fig. 4 (b), the orange arc is approximated by the connected blue links, such that each joint position P_{i-1} ($i \in \{1, 2, ..., N\}$) of the links is distributed on the arc. The local bending angle θ_i between the vertical axis of the line connecting the joint P_i of each link and $P_0 = P_{base}$ is calculated using the following equation:

$$\theta_i = \frac{\Theta_{entire}}{N} i \tag{2}$$

To obtain the local deformation, the local bending angle α_i, shown in Fig. 4 (c) by purple arrows, is utilized instead of θ_i. α_i is defined as the angle between the vertical axis and the i-th link and can be represented as follows:

$$\alpha_i = \frac{\Theta_{entire}}{N}(2i + 1) \tag{3}$$

In the next section, gripper deformation is estimated by calculating the posture of each discretized link using the model indicated in (1) and (3).

IV. DEFORMATION ESTIMATION

The deformation of a soft robotic gripper is estimated using the deformation model defined in Section III. As mentioned in Section I and shown in Fig. 1, deformation depends on both the deformation characteristics and positions of contact points. A stereo camera, which can acquire both color and depth images, was used as a sensor to obtain the information required to model or predict these factors.

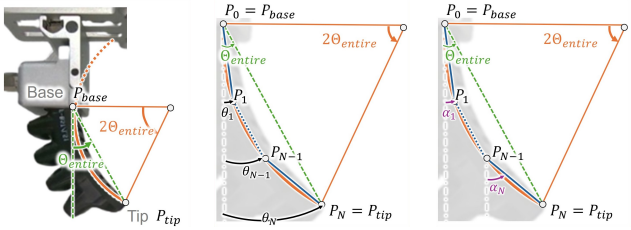

(a) Bending angle and PCC (b) Bending angle θ_i (c) Bending angle α_i

Fig. 4. Constraint conditions of the angle of each link

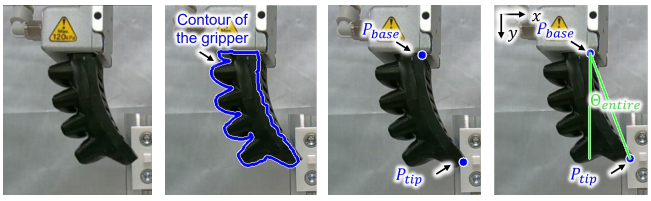

(a) (b) (c) (d)

Fig. 5. Calculation of the entire bending angle. (a) Input image, (b) Obtained contour of the object, (c) Detected base and tip points of the gripper, (d) Entire bending angle Θ_{entire}.

A. Calibration of the entire bending angle from an image

Before the estimation, the entire bending angle Θ_{entire} is obtained for calibration of the model. As described in Subsection III-B, the bending angle of the entire gripper is assumed to be constant. Although the proposed method is assumed regardless of the object shape and gripper location, Θ_{entire} varies from gripper to gripper. Therefore, obtaining Θ_{entire} for each gripper is necessary. In this calibration, the gripper is actuated when it is not in contact with the object.

The entire bending angle Θ_{entire} is calculated from an image when the gripper is deformed without grasping any object. Initially, an image is captured using a camera, as shown in Fig. 5 (a). Subsequently, the gripper region is extracted using the color and depth information obtained from the image. The contour surrounding the gripper region is then detected. The detection result just for the left one is shown by the blue line in Fig. 5 (b). The base and tip points of the gripper are calculated from the contour, as shown by the blue dots in Fig. 5 (c). As mentioned in Section III, Θ_{entire} is defined as the difference between the entire bending angle before and after deformation. Based on this definition, Θ_{entire} is calculated as the angle between the vertical line passing through the base point of the gripper and the line connecting the base and fingertip, as indicated by the green line in Fig. 5 (d). Denoting the positions of the base and fingertip joints as $P_{base} = (x_{base}, y_{base})$ and $P_{tip} = (x_{tip}, y_{tip})$, respectively, the entire bending angle Θ_{entire} is calculated as follows:

$$\Theta_{entire} = \tan^{-1}\left(\frac{x_{tip} - x_{base}}{y_{tip} - y_{base}}\right) \tag{4}$$

where the directions of the x- and y-axes are shown in the upper left of Fig. 5 (d).

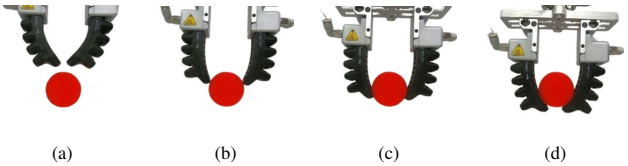

Fig. 6. Deformation cases. (a) No contact, (b) Contact only at tip, (c) Contact at the tip and another area, (d) Contact at an area other than the tip.

B. Prediction of the contact points

As described at the beginning of this section, the gripper deformation depends on the degree to which the gripper can deform and where it contacts the object. Based on these conditions, the deformation can be approximately classified into four cases, as shown in Fig. 6. Fig. 6 (a) shows the case in which the gripper and object are not in contact. The other cases are defined based on whether the contact positions correspond only to the tip (Fig. 6 (b)), the tip and another area (Fig. 6 (c)), or an area other than the tip (Fig. 6 (d)). The gripper deformation varies depending on the case, even when the same object is grasped. Thus, in this subsection, the case is first detected by predicting the contact points, and the deformation is estimated based on the case detected in the next section.

The main approach for predicting contact points is to use the contours of both the gripper and object. First, based on color and depth information, the contours of the gripper and object are extracted from Fig. 7 (a), as shown by the blue and red lines in Fig. 7 (b), respectively. In the figure, the base and tip joints of the gripper are depicted as P_{base} and P_{tip}, obtained by the same process described in Subsection IV-A. Based on these two points, the length of the entire gripper $L_{gripper}$ is calculated as follows:

$$L_{gripper} = \sqrt{(x_{base} - x_{tip})^2 + (y_{base} - y_{tip})^2} \quad (5)$$

For the gripper, only part of the contour may come into contact with the object. The part that contacts the object is extracted and approximated as a line segment between P_{base} and P_{tip}, as indicated by the blue line in the black image in Fig. 7 (c). The contour of the object is represented by a red line in the figure. Subsequently, the line connecting P_{base} and P_{tip}, shown by the blue line in Fig. 7 (c), is discretized into N rigid links. Then, each line is gradually rotated around the joint by the same angle. Specifically, the angle β_i between the vertical axis and i-th line gradually increases, as shown in Fig. 7 (d) and (e). Note that β_i is the same value for each i-th link. By continuing this rotation, the pixels corresponding to some links and the object contour may eventually overlap in the image. In Fig. 7 (f), the magenta pixels indicate overlapping contour pixels. Among the overlapping pixels, the pixel with an x-coordinate position closest to P_{base} is predicted to be the first contact point. In Fig. 7 (g), the blue and red dots P_{g1} and P_{o1} indicate the predicted positions of the first contact points on the gripper and object, respectively.

Next, based on the predicted position of the first contact point P_{g1} on the gripper, the contact case shown in Fig. 6 that will be met is determined. The distance L_{g1} between the first contact point $P_{g1} = (x_{g1}, y_{g1})$ and base point P_{base}, as indicated by the black arrow in Fig. 7 (g) can be calculated as follows:

$$L_{g1} = \sqrt{(x_{base} - x_{g1})^2 + (y_{base} - y_{g1})^2} \quad (6)$$

Then, the link N_{g1} of the total N links on the gripper that will make contact is determined by the following equation:

$$N_{g1} = \frac{L_{g1}}{L_{gripper}} N \quad (7)$$

If P_{g1} is not detected and N_{g1} cannot be calculated, then the gripper is not in contact with the object (Fig. 6 (a)). In addition, if $N_{g1} = N$, the gripper only contacts the tip (Fig. 6 (b)). If $N_{g1} < N$, then the gripper contacts either the tip and another area (Fig. 6 (c)) or an area other than the tip (Fig. 6 (d)). In the case of $N_{g1} < N$, after contacting the object at P_{g1}, the gripper may continue to deform in the closing direction. Here, this deformation is considered

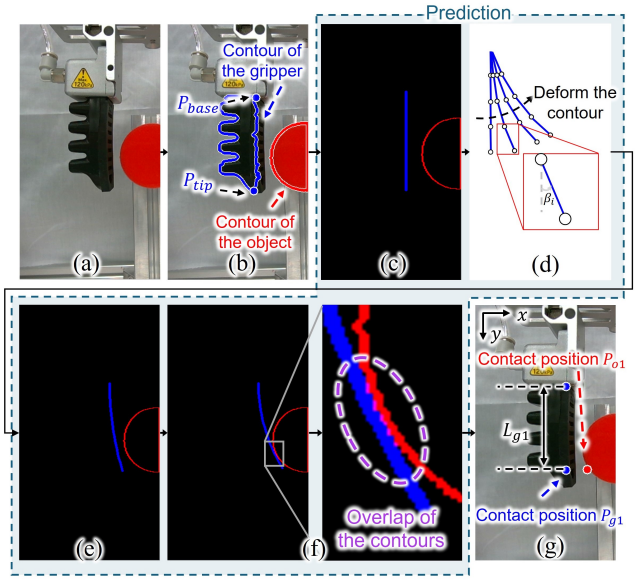

Fig. 7. Method for predicting first contact point. (a) Input image, (b) Obtained regions and joints, (c) Drawing of the contours on the black image, (d)(e) Rotating of the discretized links, (f) Overlapping of the magenta pixels of the contours, (g) Predicted first contact point for the respective gripper and object.

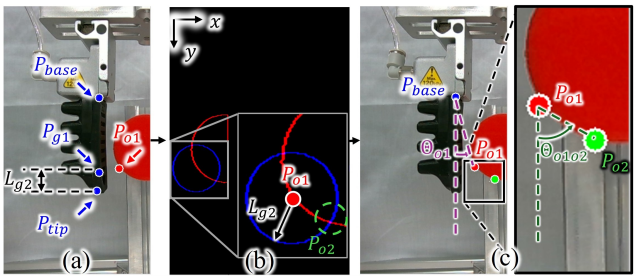

Fig. 8. Method for predicting another contact point. (a) Distance L_{g2} between P_{g1} and P_{tip}, (b) Drawing of a circle for this prediction point P_{o2}, (c) Definition of the angles Θ_{o1} and Θ_{o1o2}

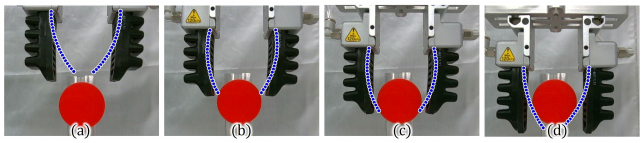

Fig. 9. Examples of the deformation-estimation result

to occur only in the region between the contact point P_{g1} and tip point P_{tip} of the gripper. Therefore, predicting this deformation and determining whether another area, in addition to the fingertip, can contact an object is necessary. This prediction determines whether the contact case is that shown in Fig. 6 (c) or Fig. 6 (d).

Another contact point is calculated based on the deformation model, that is, the length and bending angle of the gripper. First, the distance L_{g2} between the first contact point P_{g1} on the gripper and fingertip P_{tip} is calculated, as indicated by the black arrow in Fig. 8 (a). Then, a circle around the first contact point on the object with radius L_{g2} and the object contour are drawn on a black image using blue and red lines, respectively, as shown in Fig. 8 (b). Among the overlapping pixels of these two lines, the point P_{o2} whose y-coordinate position is the largest, is detected, as indicated by the green circle in Fig. 8 (b). Next, considering the entire bending angle of the gripper, it is predicted whether the tip of the gripper can be deformed to the point P_{o2}. For the prediction, two angles, Θ_{o1o2} and Θ_{remain}, are compared. Θ_{o1o2} is the angle that indicates the amount of deformation required for contact at point P_{o2} from the first contact point P_{o1}, as indicated by the green arrow in Fig. 8 (c). In addition, as shown in the figure, Θ_{o1o2} is calculated as the angle between the vertical line and the line connecting P_{o1} and P_{o2}. Θ_{remain} is the angle representing the extent to which the gripper can bend after contacting the object at the first contact point P_{g1}. To obtain Θ_{remain}, the angle Θ_{o1} is acquired as the bending angle until the first contact, as indicated by the purple arrow in Fig. 8 (c). Also depicted in the figure, Θ_{o1} is calculated as the angle between the vertical line and the line connecting P_{base} and P_{o1}. Using the entire bending angle Θ_{entire} and the angle Θ_{o1}, Θ_{remain} is calculated as follows:

$$\Theta_{remain} = \Theta_{entire} - \Theta_{o1} \tag{8}$$

If $\Theta_{remain} \geq \Theta_{o1o2}$, the gripper can be deformed by Θ_{o1o2}, and the tip of the gripper will be in contact with P_{o2}, indicating that the contact position will be at the tip and another area (Fig. 6 (c)). However, if $\Theta_{remain} < \Theta_{o1o2}$, an area other than the tip will be in contact (Fig. 6 (d)).

C. Deformation Estimation

Considering the deformation model and predicted contact positions calculated in Subsections IV-A and IV-B, the deformations of the gripper for each of the four contact cases in Fig. 6 are estimated prior to grasping. Because the deformation model (the entire length $L_{gripper}$ and bending angle Θ_{entire} of the gripper) defined in (4) and (5) is

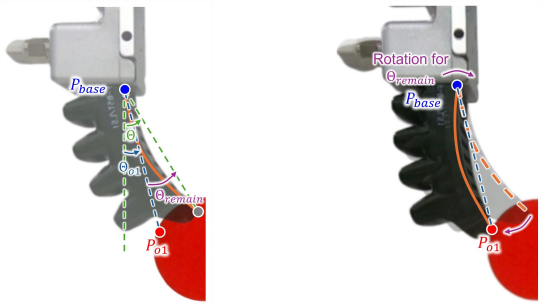

(a) (b)

Fig. 10. Deformation in the case of contact only at the tip. (a) Expected deformation when the gripper is not in contact with the object. (b) Estimated deformation.

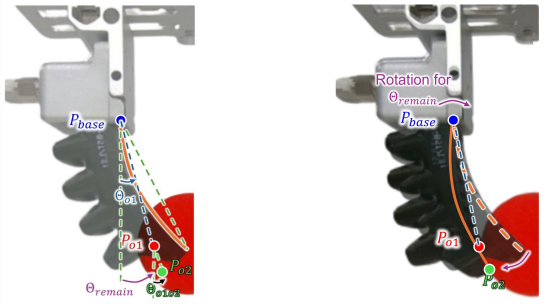

(a) (b)

Fig. 11. Deformation in the case of contact at the tip and another area. (a) Expected deformation when the gripper is not in contact with the object. (b) Estimated deformation.

calculated regardless of the contact cases, the process after these calculations is detailed with reference to Fig. 9.

First, in cases where the gripper and object are not in contact (Fig. 6 (a)), (1) and (3) are calculated for all the links, and the deformation is estimated, as shown in Fig. 9 (a).

Second, when the gripper and object are in contact only at the tip (Fig. 6 (b)), the gripper does not adapt to the shape of the object and deforms to the opposite side of the object. The gripper deforms to satisfy the condition of the entire bending angle Θ_{entire}; however, if the tip contacts an object, the gripper cannot deform toward the object side. In Fig. 10 (a), Θ_{entire} is the entire bending angle, Θ_{o1} is the bending angle until the first contact, and Θ_{remain} is the angle that represents the extent to which the gripper can bend after the first contact, as indicated by the green, blue, and purple arrows, respectively. Because the entire bending angle is constant, the gripper deforms to the opposite side of the object by angle Θ_{remain}. To estimate this deformation, the contour of the gripper shown by the orange solid arc in Fig. 10 (b) is rotated in the opposite direction by Θ_{remain} centered at P_{base}. Consequently, the estimation showed that the gripper contacts the object at P_{o1} and deforms such that the bending angle of the entire gripper is Θ_{entire}, as shown in Fig. 9 (b).

When the gripper is in contact with the tip and another area (Fig. 6 (c)), the gripper also deforms on the side

opposite the object because the tip of the gripper contacts the object, as described in a previous paragraph. As described in Subsection IV-B, the gripper is predicted to be in contact twice. Therefore, the deformable angle Θ_{remain} after contact at both P_{o1} and P_{o2}, as shown in Fig. 11 (a), is recalculated as follows:

$$\Theta_{remain} = \Theta_{entire} - \Theta_{o1} - \Theta_{o1o2} \tag{9}$$

Subsequently, the contour of the gripper is rotated by Θ_{remain} centered at P_{base}, as shown in Fig. 11 (b) and Fig. 10. Consequently, the deformation is estimated, as shown in Fig. 9 (c).

The last case occurs when the gripper makes contact with an area other than the tip. In this case, the gripper makes contact only once at P_{o1}. The links between P_{base} and P_{g1} deform to satisfy angle Θ_{o1}. The remaining links deform to satisfy Θ_{remain} in (8). However, the tip does not contact the object, as shown in Fig. 9 (d).

By considering both the deformation characteristics of the gripper and the contact points between the gripper and object, the deformation of the gripper is estimated.

V. EXPERIMENTS

Two types of experiments were conducted to verify the effectiveness of the proposed method. (A) The accuracy of the proposed estimation was quantitatively evaluated in Subsection V-A. (B) The versatility of the difference in the contact positions was qualitatively verified in Subsection V-B.

A. Quantitative-evaluation experiments

1) Evaluation method: The proposed method was evaluated quantitatively based on the error in estimating each gripper position. The error was calculated as the difference between the estimated and observed positions. The estimated positions were those of the N joints estimated using the proposed method before the gripper was actuated. The observed positions were those on the gripper contour detected after actuation and were obtained by dividing the contour into N equal parts. Denoting the estimated position of i-th joint as $P_{i,est} = (x_{i,est}, y_{i,est})$ and the observed position of the i-th joint as $P_{i,obs} = (x_{i,obs}, y_{i,obs})$, the error ϵ_i between them was calculated as follows:

$$\epsilon_i = \sqrt{(x_{i,est} - x_{i,obs})^2 + (y_{i,est} - y_{i,obs})^2} \tag{10}$$

In this study, the error ϵ_i was acquired for two points, $i = N/2$ and $i = N$, corresponding to the middle link of the entire gripper and fingertip, respectively. The mean and standard deviation of ϵ_i were evaluated for these two positions over five trials for each condition, as described in Sub-subsection V-A-2.

2) Experimental environment: The experiments were conducted in the environment shown in Fig. 12. In this experiment, DOBOT MG400 Soft Gripper Kit (Shenzhen Yuejiang Technology) was used for the soft robotic gripper, and RealSense D405 (Intel) was used for a stereo camera. The gripper length was 52 mm. The distance between the camera and gripper was 12 mm.

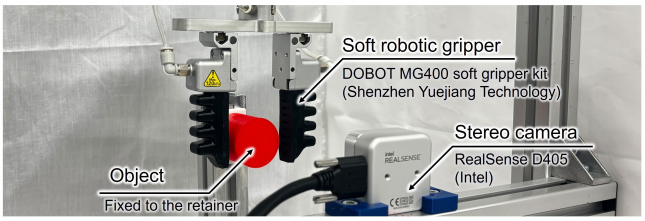

Fig. 12. Experimental environment

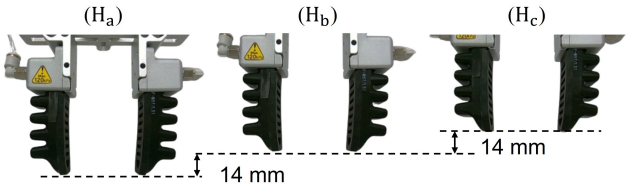

Fig. 13. Locations of the gripper

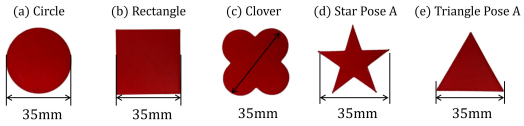

(a) Tested objects for Experiment A-b and B

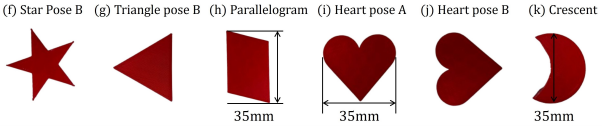

(b) Tested objects just in Experiment B

Fig. 14. Tested objects

3) Experimental conditions: Two types of experiments were conducted: Experiment A-a with no object and Experiment A-b with objects of various shapes. In both experiments, the gripper deformation was estimated when the gripper was opened and observed when it was closed. The opening and closing motions were performed five times under each of the following conditions.

In Experiment A-a, all the trials were conducted without placing any objects within the gripper. Trials were performed at each of the three gripper locations, as shown in Fig. 13. The estimation and observation were performed by changing the number N of the gripper divisions to 2, 10, and 20.

The purpose of Experiment A-b was to verify the robustness of the proposed method to contact with object and its shape. Therefore, objects with five shapes were used, as shown in Fig. 14. The objects were referred to in a paper related to object grasping [19] and were fabricated using a 3D printer with PLA plastic. In addition, the objects were fixed to the retainer such that their centroids coincided with the tip of the gripper at location H_b in Fig. 13. Similar to Experiment A-a, the gripper location varied for each object.

4) Results and discussion for Experiment A-a with no object: The experimental results are presented in Table I. The results were computed from ϵ_i obtained at all locations H_a, H_b and H_c. Examples of the results for links N = 2, 10,

TABLE I. Estimation errors in experiment A-a

N	i	Mean [mm]	Standard deviation [mm]
2	1	0.77	0.42
	2	0.99	0.40
10	5	0.80	0.33
	10	0.96	0.44
20	10	0.79	0.30
	20	0.96	0.31

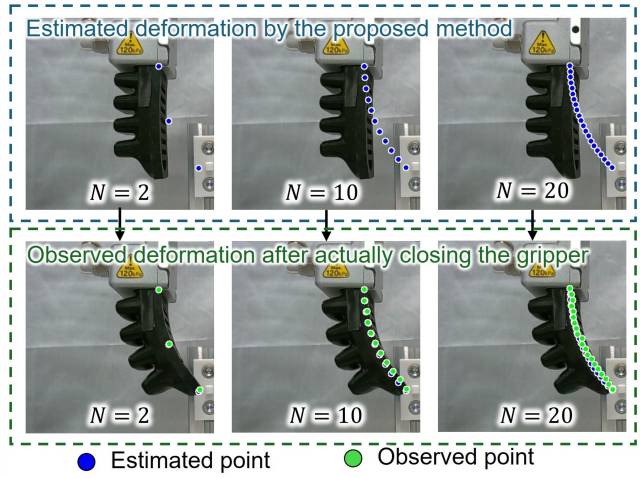

Fig. 15. Examples of the results for Experiment A-a without object; (Top) Results of the proposed estimation of the deformation before the actuation, and (Bottom) Results of the observation after actually closing the gripper.

and 20 at location H_b are shown in Fig. 15. In the upper part of the figure, the blue dots indicate the estimation results of the proposed method before the gripper is closed. The lower part of the figure shows the observed points when the gripper was closed and the estimated points as green and blue dots, respectively.

The results show that the mean and standard deviation of the estimation error were both less than 1 mm and 0.5 mm, respectively. This indicates that the deformations were estimated with high accuracy and repeatability. In the experiment, the gripper could be considered deformed simply by its deformation characteristics (e.g., stiffness) because no object was contacted in the experiments. Thus, the proposed approaches described in Section IV were valid for modeling the deformation characteristics of the gripper.

Because no significant differences were observed in the estimation error and repeatability, regardless of the number of N, Experiment A-b was performed using the largest number of discretization: N = 20.

5) Results and discussion for Experiment A-b with object: The experimental results are presented in Table II. The results were computed from ϵ_i obtained at all locations H_a, H_b and H_c. Fig. 16 presents examples of the results for each of the five objects at location H_b. In Fig. 16, the upper and lower parts of the figure represent the deformation estimated using the proposed method and observed deformation, respectively.

The results shows that the mean of the estimation error was from 0.96 mm to 2.46 mm, and the standard deviation was from 0.22 mm to 1.38 mm, which are larger values

TABLE II. Estimation errors in experiment A-b for $N = 20$

Object	i	Mean [mm]	Standard deviation [mm]
(a) Circle	10	1.92	0.25
	20	1.47	0.25
(b) Square	10	2.46	0.59
	20	1.09	0.28
(c) Clover	10	1.72	0.22
	20	1.41	0.37
(d) Star (Pose A)	10	2.03	0.42
	20	2.63	1.38
(e) Triangle (PoseA)	10	1.57	0.44
	20	0.96	0.49

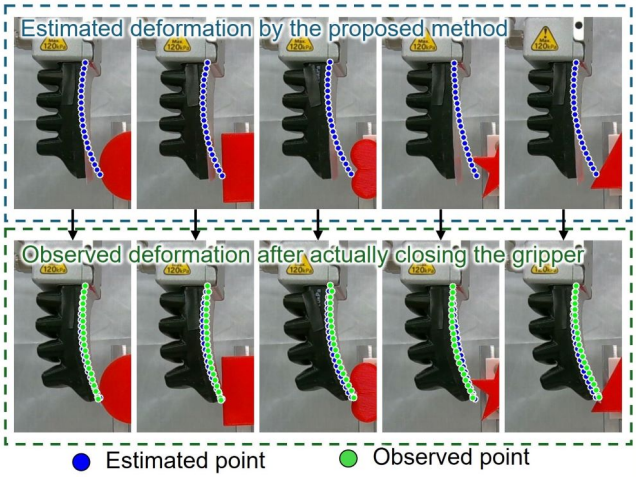

Fig. 16. Examples of the results for Experiment A-b with five objects. (Top) Results of the proposed estimation of the deformation before the actuation, (Bottom) Results of the observation after actually closing the gripper.

than those of Experiment A-a. The estimation errors was considered to increased overall owing to the shrinkage of the soft robotic gripper after contact. In Fig. 16, the curvature produced by the observed points appeared to be more gradual than that produced by the estimated points. Because the gripper was made of a flexible material, it could be shrunk by the grasping force exerted after contact. Therefore, the entire bending angle, which indicates the curvature, may have changed. However, because of the adaptability of soft robotic grippers, these estimation errors can be absorbed. Therefore, we first evaluate the effects of these estimation errors on grasping stability. Based on the evaluation, the estimation after contact was revised by considering shrinkage.

B. Qualitative-evaluation experiment

To qualitatively verify the versatility of the proposed method for different contact positions, deformation estimations were conducted for 11 types of objects, as shown in Fig. 14 (a) and (b). The estimation results were confirmed visually. For experimental conditions other than the object shapes, the same setups and conditions of the gripper locations were applied, as in Experiment A-b.

The experimental results are presented in Fig. 17. The results of the estimated points are overdrawn as blue dots on the images after contact with the objects. This indicates

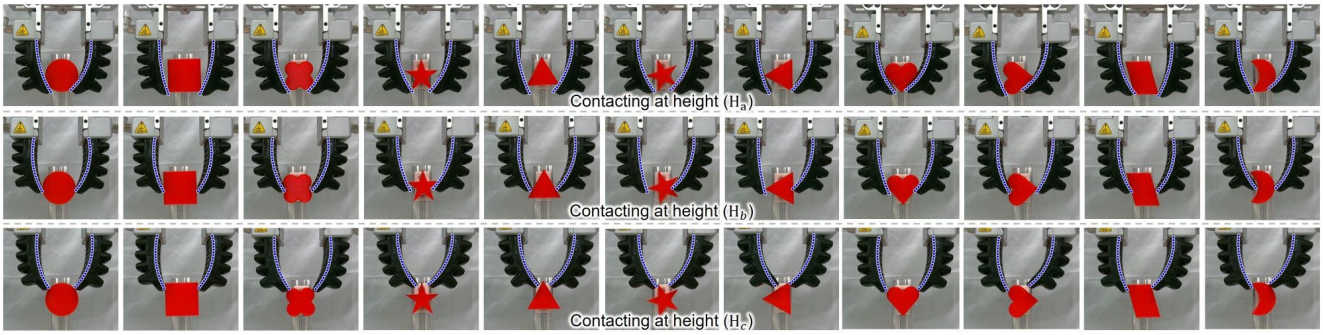

Fig. 17. Results for experiment B. The results estimated before contact with objects are overdrawn as blue dots on the image captured after the contact.

that the deformation estimation appears to work well under most conditions. This suggests that the proposed method can be applied to a wide range of objects and contact positions. Although the proposed method is used as a pre-touch estimation, a pre-touch motion that can adjust the gripper location to grasp the object stably is also required. In future work, we will consider combining the proposed estimation with the method to evaluate the grasping stability based on the deformation of the gripper, as in [11], [12], and develop the motion based on this combination.

VI. CONCLUSION

In this study, a vision-based method for estimating the deformation of a soft robotic gripper before grasping an object was proposed. In the proposed method, the deformation of the gripper was first modeled using three approaches: discretization using *a model of a serial chain of rigid bodies connected with spring joints*, bending angle, and PCC. First, the entire bending angle was calculated from an image acquired using a stereo camera for calibration. Subsequently, the contact points were predicted based on the contours of the gripper and object using a camera image. Afterwards, gripper deformation was estimated by considering the deformation model and predicted contact points. In the experiments, the deformation of the soft robotic gripper was estimated using the proposed method when the object or gripper location varied. Through experiments, the mean estimation error obtained was less than 2.5 mm. Thus, we concluded that the proposed method could estimate the gripper deformation before grasping under various conditions.

In the future, we will evaluate the grasping stability using the proposed estimation and then realize the pre-touch motion of a soft robotic gripper by combining the estimation and evaluation.

REFERENCES

[1] J. Shintake *et al.*, "Soft Robotic Grippers", Advanced Materials, Vol. 30, No. 29, pp. 170735, 2018.

[2] Valuates Reports, "Global Soft Robotic Gripper Market Research Report 2023," https://reports.valuates.com/ https://reports.valuates.com/market-reports/QYRE-Auto-37Q14112/global-soft-robotic-gripper Accessed on Febuary 17, 2024.

[3] W. Park *et al.*, "A Sensorized Hybrid Gripper to Evaluate a Grasping Quality Based on a Largest Minimum Wrench," in IEEE Robotics and Automation Letters, Vol. 5, No. 2, pp. 3243–3250, 2020.

[4] K. Harada *et al.*, "Stability of soft-finger grasp under gravity," IEEE Int. Conf. on Robotics and Automation (ICRA), pp. 883–888, 2014.

[5] P. M. Khin *et al.*, "Development and Grasp Stability Estimation of Sensorized Soft Robotic Hand," Frontiers in Robotics and AI, Vol. 8, 2021.

[6] M. V. Liarokapis and A. M. Dollar, "Post-Contact, In-Hand Object Motion Compensation With Adaptive Hands," in IEEE Trans. on Automation Science and Engineering, Vol. 15, No. 2, pp. 456–467, 2018.

[7] M. Bowman and X. Zhang, "Dynamic Pre-Grasp Planning when Tracing a Moving Object Through a Multi-Agent Perspective," IEEE/RSJ Int. Conf. on Intelligent Robots and Systems (IROS), pp. 9408–9414, 2021.

[8] B. Yang *et al.*, "Pre-touch sensing for sequential manipulation," IEEE Int. Conf. on Robotics and Automation (ICRA), pp. 5088–5095, 2017.

[9] Y. Hirai *et al.*, "High-Speed and Intelligent Pre-Grasp Motion by a Robotic Hand Equipped with Hierarchical Proximity Sensors," IEEE/RSJ Int. Conf. on Intelligent Robots and Systems (IROS), pp. 7424–7431, 2018.

[10] S. Rupavatharam *et al.*, "SonicFinger: Pre-touch and Contact Detection Tactile Sensor for Reactive Pregrasping," IEEE Int. Conf. on Robotics and Automation (ICRA), pp. 12556–12562, 2023.

[11] J. Li *et al.*, "Marker-Based Shape Estimation of a Continuum Manipulator Using Binocular Vision and Its Error Compensation," IEEE Int. Conf. on Mechatronics and Automation (ICMA), pp. 1745–1750, 2020.

[12] H. N. Le *et al.*, "Behavior Analysis of Soft Pneumatic Actuator Gripper by using Image Processing Technology," IEEE Int. Conf. on Mechatronics and Automation (ICMA), pp. 1798–1802, 2020.

[13] C. Choi *et al.*, "Learning Object Grasping for Soft Robot Hands," in IEEE Robotics and Automation Letters, Vol. 3, No. 3, pp. 2370–2377, 2018.

[14] V. Vatsal and N. George, "Augmenting Vision-Based Grasp Plans for Soft Robotic Grippers using Reinforcement Learning," IEEE Int. Conf. on Automation Science and Engineering (CASE), pp. 1904–1909, 2022.

[15] C. Agabiti *et al.*, "Whole-arm Grasping Strategy for Soft Arms to Capture Space Debris," IEEE Int. Conf. on Soft Robotics (RoboSoft), pp. 1–6, 2023.

[16] K. Suzumori *et al.*, "The Science of Soft Robots: Design, Materials and Information Processing," Springer, 2023.

[17] Q. Jiang and F. Xu, "Design and Motion Analysis of Adjustable Pneumatic Soft Manipulator for Grasping Objects," in IEEE Access, Vol. 8, pp. 191920–191929, 2020.

[18] R. Webster III *et al.*, "Design and kinematic modeling of constant curvature continuum robots: A review", The Int. Journal of Robotics Research, Vol. 29, No. 13, pp. 1661-–1683, 2010.

[19] Y. Isobe *et al.*, "Vision-Based In-Hand Manipulation of Variously Shaped Objects via Contact Point Prediction," IEEE/RSJ Int. Conf. on Intelligent Robots and Systems (IROS), pp. 8727–8734, 2023,